Fermi National Accelerator Laboratory

FERMILAB-Conf-91/291

Scintillating plastic optical fiber radiation detectors in high energy particle physics

A. D. Bross

Fermi National Accelerator Laboratory
P.O. Box 500, Batavia, Illinois 60510

October 1991

* Presented at the *SPIE Conference on Optical Fiber Technology*, Boston, Massachusetts, September, 1991.

Scintillating plastic optical fiber radiation detectors in high energy particle physics

Alan D. Bross
Detector Group
Fermi National Accelerator Laboratory

October 26, 1991

Abstract

We describe the application of scintillating optical fiber in instrumentation for high energy particle physics. The basic physics of the scintillation process in polymers is discussed first and then we outline the fundamentals of scintillating fiber technology. Fiber performance, optimization, and characterization measurements are given. Detector applications in the areas of particle tracking and particle energy determination are then described.

Talk presented at the SPIE Conference on Optical Fiber Technology, Boston, Massachusetts, September, 1991. To be published in the proceedings of the SPIE.

Scintillating plastic optical fiber radiation detectors in high energy particle physics

Alan D. Bross

Fermi National Accelerator Laboratory
Batavia, IL 60510

ABSTRACT

We describe the application of scintillating plastic optical fiber in instrumentation for high energy particle physics. The basic physics of the scintillation process in polymers is discussed first and then we outline the fundamentals of scintillating fiber technology. Fiber performance, optimization, and characterization measurements are given. Detector applications in the areas of particle tracking and particle energy determination are then described.

1 INTRODUCTION

Recently, there has been a renewed interest in plastic scintillators for detector applications in high energy particle physics. Much of this has been driven by the development of high-quality plastic scintillating optical fiber which, in turn, has given birth to a whole new generation of scintillation detectors.

These detectors are primarily concerned with the measurement of the trajectories and energies of ultra-relativistic particles. From the point of view of their interaction in matter and subsequent detection, these particles can be divided into the following classes:

1. Heavy ionizing radiation: protons, pions.
2. Electrons or positrons.
3. Electromagnetic radiation: photons, π°.
4. Neutrons.

The physical processes that govern particle interaction with matter are:

1. Ionization loss, dE/dx, for charged particles.
2. Bremmstralung (photon emission) for electrons.
3. Compton scattering, the photoelectric effect, and pair production for photons.

In all cases, however, energy is eventually transferred to the polymer base of the scintillator and this excitation energy leads to the emission of light (fluorescence), which is the detected signal.

Scintillating plastic optical fiber is based on stepped-index optical fiber technology. Most applications use polystyrene ($n_F = 1.61$) as the core material and polymethylmathacrylate ($n_F = 1.48$) as the cladding.

2 PHYSICS OF THE SCINTILLATION PROCESS IN POLYSTYRENE

The physics of the scintillation process in polystyrene and in all organic materials is essentially governed by the electronic structure of the carbon atom which in the ground state is: $1s^2 2s^2 2p^2$. In the formation of hydrocarbons, the carbon atoms are considered to be in an excited state leading to a "hybridized" orbital structure, $1s2s2p^3$, with one π orbital and three σ orbitals. The free electron model of Platt[1] treats the π orbitals as fully delocalized about the perimeter of a polycyclic molecule. The theory then introduces a π orbital wave function that is periodic and results in discrete energy levels for π electrons.

2.1 Intrinsic fluorescence - scintillation

In aromatic compounds like polystyrene, it is the excitation of π-orbital electrons and their transition between discrete energy levels that leads to fluorescence. Fluorescence is defined as the radiative transition from the first excited singlet state to the ground state,

$$S_1 \rightsquigarrow S_0$$

with the emission of a photon. Excitation of π-electrons by ionizing radiation and the subsequent fluorescence of the excited states is the principal energy transfer process in organic scintillators. The primary scintillation efficiency, P, is just the fraction of the energy deposited in the scintillator that goes into π-electron excitation. For most aromatics, $P \simeq 0.1$. However, not all of this excitation energy leads to fluorescence. A number of non-radiative de-excitation processes can compete with fluorescence. Internal quenching, in which the excitation energy is dissipated non-radiatively, has a large rate constant in polystyrene and thus the radiative quantum yield (probability of fluorescence) in polystyrene is only 7%.[2]

2.2 Energy-couplers

Solutions of polystyrene plus an efficient fluorescent dopant can give a system with close to unity quantum yield, however. Quantum yield in this case is defined as the probability that an excited state in the polymer leads to the emission of a photon by a dopant through the process:

$$D^* + A \rightarrow D + A^* \rightarrow D + A + \gamma.$$

where D is the polystyrene (donor), A the dopant (acceptor), and the * refers to an excited state. A theory of non-radiative energy transfer between molecules in solution has been developed by Förster.[3] The energy transfer is described by a dipole-dipole interaction in which non-radiative energy transfer occurs between the first excited π-singlet state of the solvent (polystyrene in this case) and the solute (dopant). The strength of this interaction is

$$k = \frac{1}{(\tau_{0s})_0}\left(\frac{R_0}{r}\right)^6$$

where $(\tau_{0s})_0$ is the natural fluorescence lifetime of the solvent, r is the mean separation between solvent and solute molecules and R_0 is a constant proportional to the overlap integral between the solvent fluorescence distribution and the solute absorption:

$$R_0^6 \propto \int_0^\infty f_s(\nu)\epsilon_d(\nu)\frac{d\nu}{\nu^4}.$$

ν is the wavenumber, $f_s(\nu)$ the solvent fluorescence distribution and $\epsilon_d(\nu)$ the absorption distribution of the solute. Typical values for R_0 in polystyrene systems are between 5 and 30 Å.[4] At high dopant concentration (r small compared to R_0) this process can dominate over emission or quenching of the solvent. Thus if the dopant's radiative quantum yield is close to unity, the number of photons emitted per solvent molecule π-electron excitation can approach one, even though the radiative quantum yield of the solvent may be small.

2.3 Single vs. multiple step systems

Dopants added in high concentration ($\simeq$ 1%) that couple to the primary scintillation of the solvent are referred to as primary dopants. They both raise the scintillation photon yield (the number of photons emitted per unit energy deposited in the solvent) and shift the mean wavelength of the final fluorescence to longer wavelength. A binary system, solvent (polystyrene) plus primary dopant, can be considered a single step or intrinsic scintillator because the dopant couples directly to the primary scintillation on a distance scale of Angstroms.

Secondary dopants may also be added, but their function is qualitatively different from that of the primary. Secondary dopants are typically added in low concentration ($\simeq$ 0.01%) and only shift the mean fluorescence wavelength further into the red. They do not increase the intrinsic photon yield of the scintillator. Energy transfer between the primary and secondary dopant is through the emission and reabsorption of a photon (the trivial process). At best, this process can only maintain the photon yield of the primary. Secondary dopants increase the technical photon yield of a scintillator, however. By shifting the fluorescence emission to longer wavelength, more of these photons can escape from finite sized scintillators and, self-absorption by the scintillator is thus reduced. Most primaries used in polystyrene based scintillators fluoresce in the deep blue, $\lambda_p \simeq$ 350 - 390 nm. As can be seen in Figure 1, polystyrene absorbs quite strongly in this spectral region. Without the use of a secondary dopant, much of the light produced by the primary is reabsorbed within a few centimeters. Although the use of a secondary wavelength shifter does increase the technical quantum yield of a scintillator, the process of emission by the primary, followed by absorption by the secondary, and finally by emission from the secondary, does not give unity photon yield. Self-absorption by the primary and by the secondary lead to a decrease in yield, since rarely do these dopants have quantum yields of one. It is the finite overlap between the absorption and emission spectra of the various dopants that leads to these efficiency losses. In particular, for very large path lengths within the scintillator, self-absorption losses by the secondary can become quite substantial.

2.4 Intra-molecular proton transfer compounds

Ideally one would like to use wavelength shifters whose emission and absorption spectra have no overlap. Compounds which undergo intra-molecular proton transfer (IPT) upon excitation exhibit this property.[5] Renschler and Harrah first reported using 3-hydroxyflavone (3HF) in polyvinyltoluene based scintillators.[6] In their studies, 3HF was used as an intermediate wavelength shifter between the primary and the terminal wavelength shifter. It was then

proposed that since 3HF's absorption spectrum overlapped the fluorescence emission distribution for polystyrene, 3HF (or other IPT compounds with appropriate absorption spectra) could be used as the primary dopant in polystyrene based scintillators if it could be added in sufficient concentration.[7] In addition, since the fluorescence distributions for these types of compounds have emission peaks at wavelengths often longer than 500nm, no secondary dopant would be required. For the use in plastic scintillating optical fiber, this situation is ideal. We have a single step system (binary) in which the light produced by ionization is localized along the track trajectory to within approximately 10-20 Å. Energy transfer is very efficient since the only transfer is via the Förster mechanism, and there should be little self-absorption by the dopant. Also, the final fluorescence is in a wavelength region where polystyrene is extremely transparent. Figure 2 shows the absorbance and fluorescence distributions for two derivatives of 3HF, 2-methyl-3HF and 4-phenyl-3HF. As can be easily seen, there is essentially no overlap between absorption and emission, and the peak fluorescence of both compounds is in a region where polystyrene absorption is extremely small.

3 SCINTILLATING FIBER FUNDAMENTALS

As mentioned in the introduction, scintillating fiber is based on stepped-index optical fiber technology. Even though a polystyrene core, acrylic clad fiber has a relatively high numerical aperture of 0.63, the fraction of light produced in the fiber that is piped in either direction is relatively small. This is illustrated in Figure 3. Only light that is emitted within a cone of half angle 90-θ_c, where θ_c is the critical angle ($\sin\theta_c = n_{clad}/n_{core}$) is piped in each direction in the fiber. It is simple to show that the fraction of total light produced that is piped in each direction is then just equal to $0.5(1\text{-}n_{clad}/n_{core})$. For a fiber with a polystyrene core and an acrylic clad this "piping efficiency" is just 3.8%.

3.1 Scintillating fiber performance

Typical polystyrene scintillator has an overall scintillation efficiency, the fraction of energy deposited in the polymer that is emitted as visible light, of approximately 3%. This corresponds to an emission of 10 photons for each KeV of deposited energy. A minimum ionizing particle deposits 1.7 MeV/cm in polystyrene, so for a 1 mm fiber, approximately 1700 photons are emitted. Using the 3.8% piping efficiency given above, we find that roughly 65 photons are piped in each direction in the fiber.

Attenuation effects in scintillating fiber are characterized by, bulk absorption, Rayleigh scattering, and interface losses. Attenuation lengths (1/e) have been measured to be as long as 4 m in the spectral region around 450 nm and up to 9 m for wavelengths longer than 500 nm. In order to optimize the waveguide properties of scintillating fiber, we must have a precise technique to evaluate their performance. Attenuation studies are performed in order to measure the attenuation as a function of wavelength where the attenuation is described by:

$$A(\lambda) \propto exp(-L/\alpha(\lambda))R(\lambda)^{tan\theta(L/d)}$$

and $\alpha(\lambda)$ is the wavelength dependent bulk absorption coefficient, $R(\lambda)$ is the reflection coefficient, L is the distance in the fiber from the point of excitation to the detector end, θ is the reflection angle for a given photon, and d is the diameter of the fiber. The system we use for the these measurements is shown in Figure 4. It consists of an ISA model HR 320 monochrometer coupled to a Princeton Instrument's IRY700 intensified diode array detector head. The IRY700 uses a micro-channel plate intensifier that has a S-20 photocathode. With a 147 groove/mm grating, this system gave approximately 0.5 nm resolution/diode. Measurements were made by exciting the fiber with a UV source at source positions from 10 cm to 5 m from the fiber end. Light from the fiber was coupled into the entrance optics of the monochrometer with a spherical lens. This arrangement more closely matched the numerical aperture of the fiber to that of the monochrometer. The procedure for parameterizing the attenuation performance of a fiber then consisted of first measuring the fluorescence distribution as a function of the distance from the excitation point to the detector end of the fiber, binning the data in wavelength bins, plotting wavelength binned signal as a function of distance, and finally fitting these data to the functional form for the attenuation given above integrated over all angles. The resulting fit gives the parameters $\alpha(\lambda)$ and $R(\lambda)$. Fluorescence data as a function of position for a typical fiber are shown in Figure 5. All monochrometer data are corrected for the wavelength dependent throughput of the monochrometer and the quantum efficiency of the IRY700. Therefore, data (as shown in Figure 5) are proportional to the true number of photons/wavelength bin exiting the fiber. The results for $\alpha(\lambda)$ and for $R(\lambda)$ are given in Figures 6 and 7. As can be seen, fibers whose fluorescence emission is in the green will have significantly better attenuation properties than those that emit in the deep blue.

4 DETECTOR APPLICATIONS

There are two principal applications in high energy physics for scintillating optical fiber detectors. The first is for tracking detectors whose purpose is to measure the positions and trajectories of particles. See Figure 8. In these detectors, a photodetector senses light produced in a single fiber. As was described above, as many as 65 photons may be piped down the fiber, but after attenuation effects are considered and the quantum efficiency of the photodetector is included, the actual signal for a single track can be as small as 5 to 10 electrons. The second major application is in calorimetry. In this case, the total energy of a particle or group of particles is measured. By embedding the fibers in an absorber such as lead, a small fraction of the total energy of the incident particle is deposited in the fiber scintillator. The signal, however, is quite large since the incident particle looses its entire energy in the absorber in a showering process that produces many secondary particles. Typical signals can be from hundreds to tens of thousands of electrons.

4.1 Tracking detectors

To date, only one large system is in operation. This detector was built by the UA2 collaboration[8] using fiber supplied by Optectron.[9] A schematic picture of the detector is shown in Figure 9. It used 1 mm diameter fiber incorporating a polystyrene scintillator core and polyvinyl acetate cladding. The fiber layers were arranged in 8 layers of stereo triplets, 0° and

$\pm 15.75°$. The active length of the detector was 2.1 m. The total number of channels was 60k and was read out using a 3 stage image intensifier coupled to a CCD with fast clear.[10]

A number of new detectors is in the design stage and most will be based on a cylindrical staggered-layer structure,[11] Figure 10. The scale of some of these designs is much larger than the UA2 detector, incorporating up to 1 million channels and up to 20k kilometers of fiber. The intensified CCD approach will not be applicable for future experiments due to the relatively long readout time involved with the CCD. Instead, avalanche photodiodes (APD's)[12] are being studied as discrete detectors for each fiber. They have the advantage of high quantum efficiency in the wavelength region (500-600 nm) of interest for most scintillating fiber tracker applications and have demonstrated single photon detection capability.

4.2 Calorimeters

The calorimeter application in high energy physics is far more widespread at this time with a number of detector systems already in operation. Since the photon yield is quite large in most experiments, conventional photomultiplier tubes (PMT) can be used as the readout device. All scintillator calorimeters use a heavy absorber such as lead or steel to stop the incident particles. The scintillator can be installed in a number of ways, usually using one of three principal geometries. The first employs layers of scintillator and absorber plates. The light produced in the plate is read out by a wavelength shifting fiber. This fiber is doped with a dye that absorbs the scintillation light in the plate and then emits fluorescence photons, a fraction of which are piped along the readout fiber to the photodetector. A picture of a prototype detector of this design built for the Collider Detector Facility at Fermilab is given in Figure 11. In it we see the layered structure of scintillator plate and absorber plate (in this case, lead). The readout wavelength shifting fiber can be seen running along the front face of the device to the back end (left hand side of the picture) of the detector. The second approach for scintillator calorimeters uses a fiber/absorber composite,[13] Figure 12. In this case, scintillating fibers are laminated to absorber plates to form a fiber/absorber matrix. The scintillating fibers are grouped together at the back end of the detector and then coupled to a PMT through a light guide. The third approach is a combination of the first two. In this case, fiber ribbons are sandwiched between flat absorber plates. Each of these techniques has particular advantages for a given geometry. For example, if very thin scintillator layers are needed then the fiber ribbon approach is preferred over the plate/wavelength shifter fiber design, since thin plates are difficult to manufacture and exhibit relatively large attenuation within the plate. The fiber/composite approach is particularly attractive if no readout segmentation is needed along the length of the fiber. The amount of fiber required in the wavelength shifter fiber approach is less than 10% of that required in the other approaches. This can be an important cost consideration , since in a large calorimeter detector system as much as 100 million meters of fiber would be required in the fiber/composite or fiber ribbon designs.

5 CONCLUSIONS

In general, scintillating plastic optical fiber technology looks very promising for many detector applications in high energy physics. Already, several calorimeters have been built

and are in operation, one fiber tracker has been successfully operated, and design studies of larger and more elaborate fiber trackers are being aggressively pursued. Areas of future R&D for scintillating fiber include: 1. New dopants for low self-absorption scintillators emitting in the green; 2. Single step scintillator systems for improved photon yield; and 3. Optical fiber/waveguide optimization addressing an interest in new cladding materials for higher light piping efficiency in the fiber and lower interface losses. In addition, investigation of new readout technologies, especially for fiber trackers, is underway at a number of institutions with special emphasis being placed on studies of new solid state photodetectors that have single photon detection capability.

References

1. J.R. Platt, *Chemical Physics*, **17**, 484 (1949).
2. J. B. Birks, *The Theory and Practice of Scintillation Counting,* (Pergamon Press, New York), (1964).
3. Förster, Th., *Comparative Effects of Radiation,* ed., M. Burton, J.S. Kirby-Smith and J.L. Magee, (John Wiley, New York), (1960).
4. J.B. Berlman, *Handbook of Fluorescence Spectra of Aromatic Molecules,* Second ed., (Academic Press, New York), (1971).
5. David L. Williams and Adam Heller, *Journal of Physical Chemistry*, **Vol. 74**, No. 26, 4473 (1970).
6. Clifford L. Renschler and Larry A. Harrah, *Nuclear Instruments and Methods in Physics Research*, **A235**, 41 (1985).
7. A.D. Bross in *Proceedings of the Workshop on New Solid State Devices for High Energy Physics,* October 20-30, (1985), LBL 22778.
8. J. Allitti, et. al., *Nuclear Instruments and Methods in Physics Research*, **A279**, 364 (1989).
9. Optectron SA, France.
10. R.E. Ansorge, et. al., *Nuclear Instruments and Methods in Physics Research*, **A265**, 33 (1988).
11. Barrel Tracker Design Report, Solenoidal Detector Collaboration.
12. Currently, devices from EG&G Canada LTD. and from Rockwell International are being studied.
13. D.W. Hertzog, et. al., *Nuclear Instruments and Methods in Physics Research*, **A294**, 446 (1990).

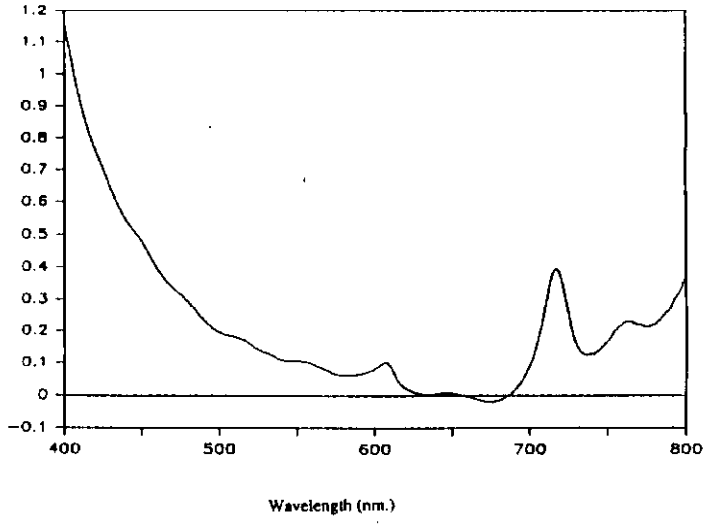

Figure 1: Absorption spectrum for polystyrene. The vertical scale is in absorption units and the data is for 1 m of fiber.

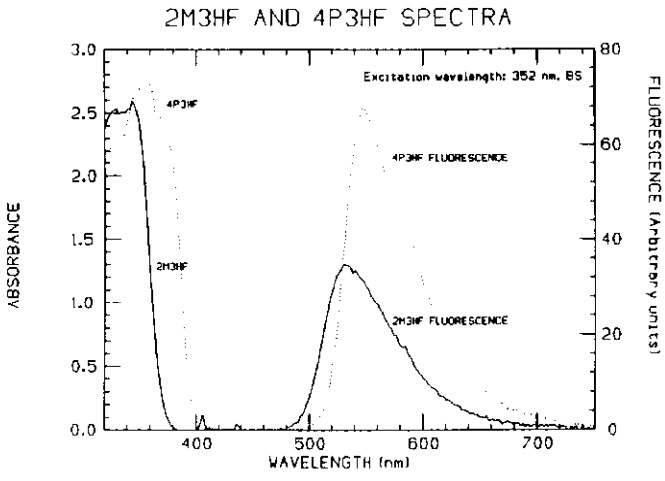

Figure 2: Absorption and fluorescence spectra for 2-methyl and 4-phenyl 3HF.

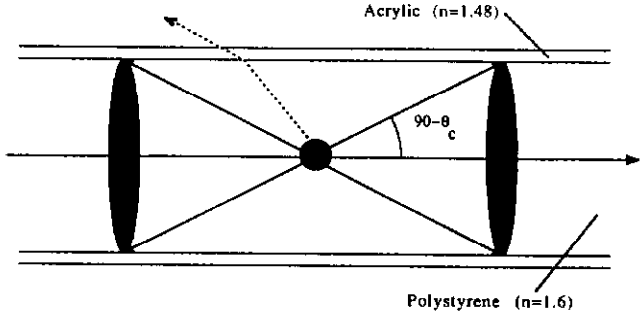

Figure 3: Light piping acceptance cones for light generated in the core of a scintillating optical fiber.

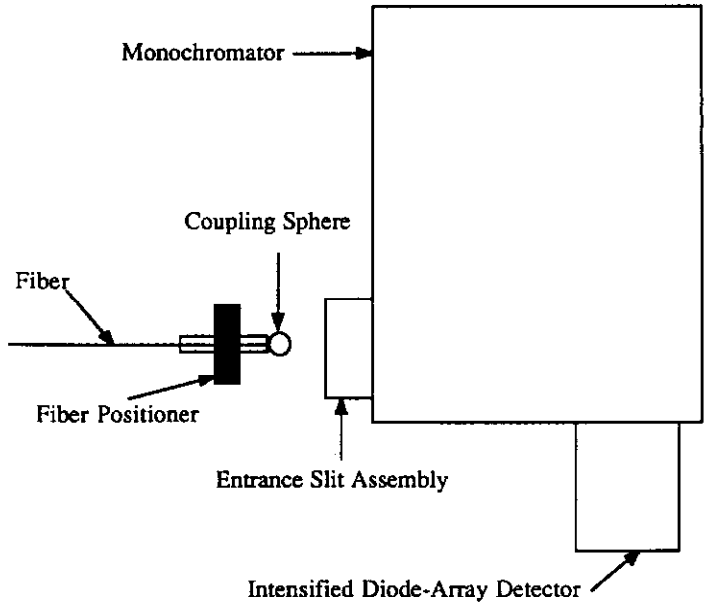

Figure 4: Schematic of monochrometer system used for fiber attenuation studies.

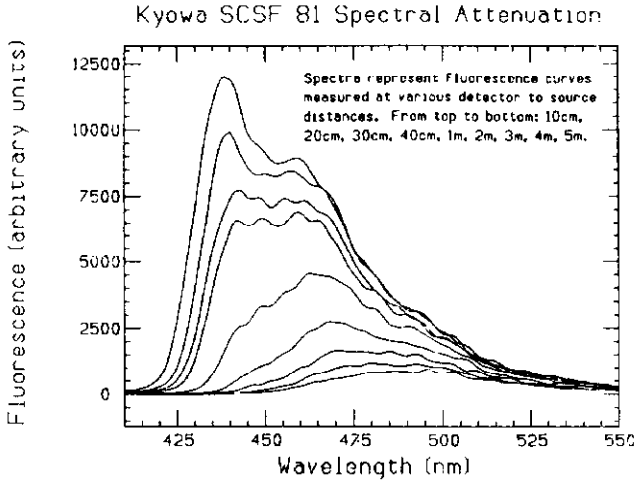

Figure 5: Fluorescence data as a function of position.

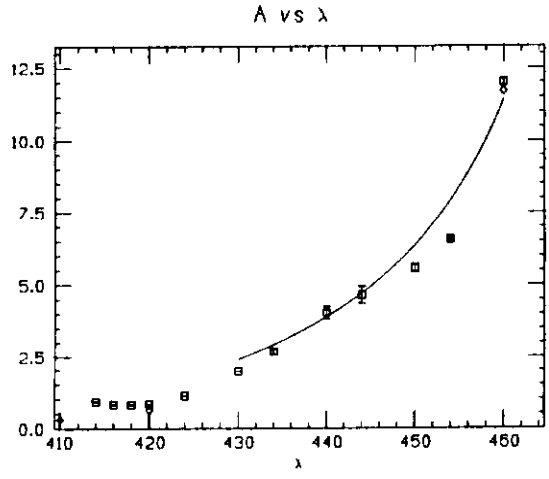

Figure 6: Wavelength dependent bulk absorption coefficient data.

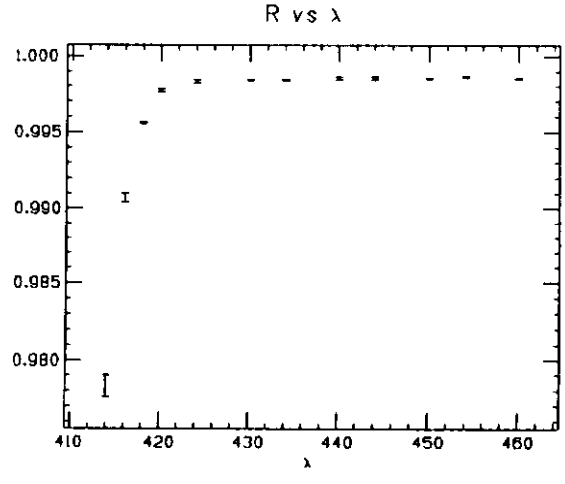

Figure 7: Wavelength dependent reflection coefficient data.

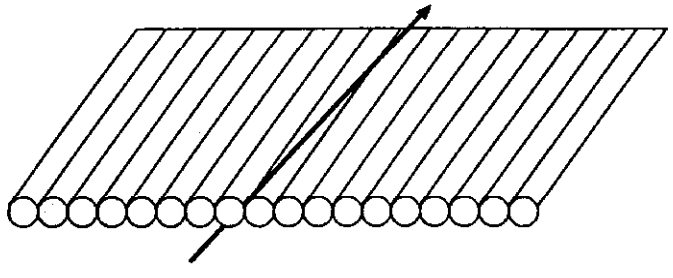

Figure 8: Fiber tracker schematic diagram.

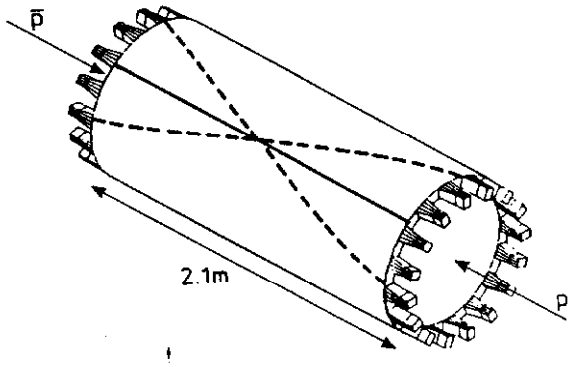

Figure 9: UA2 fiber tracker.

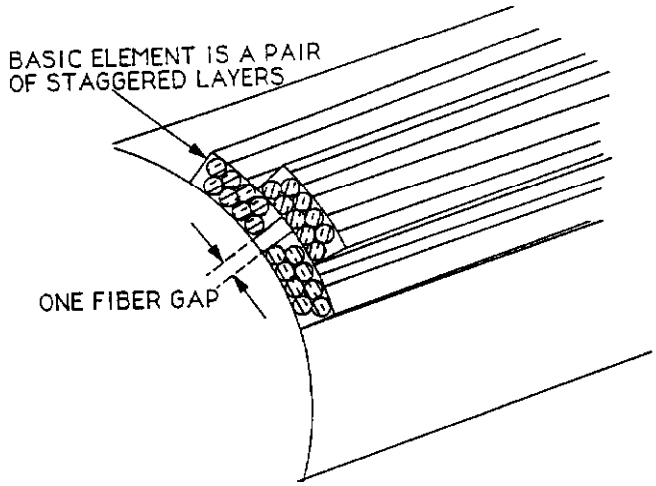

Figure 10: Basic cylindrical fiber tracker staggered-layer design.

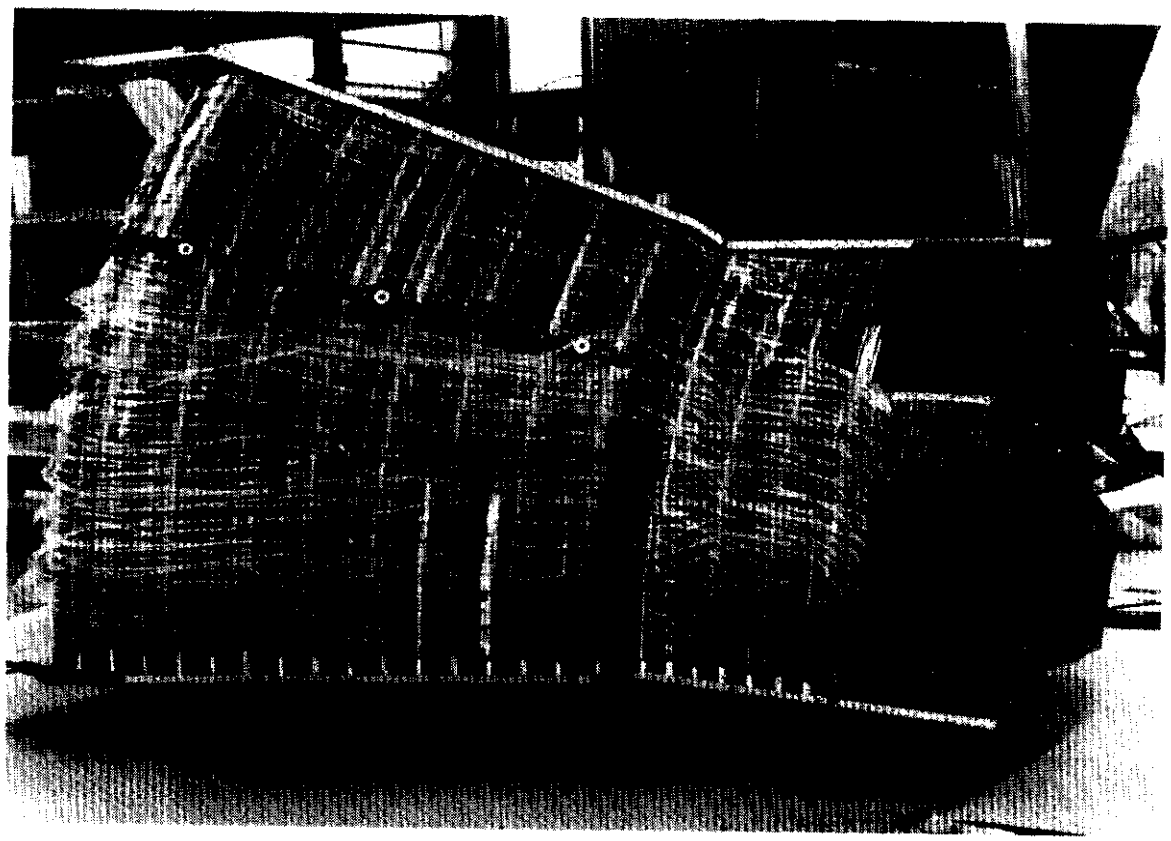

Figure 11: Collider Detector Facility scintillator/wavelength shifting calorimeter prototype.

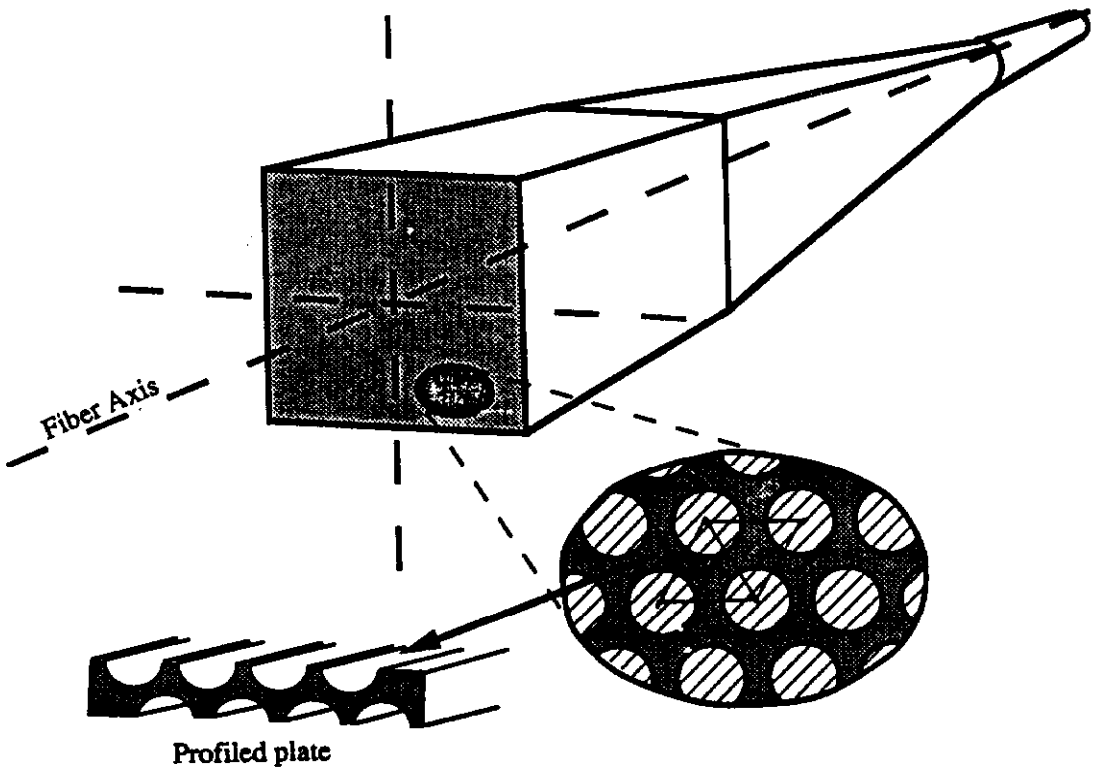

Figure 12: Fiber/absorber composite calorimeter design showing fiber, profiled absorber plate, light guide and PMT.